

Supplementary Information

Distinct Feedforward and Intrinsic Neurons in Posterior Inferotemporal Cortex Revealed by *in Vivo* Connection Imaging

Noritaka Ichinohe^{1,2,*}, Elena Borra² and Kathleen Rockland²

¹Department of Ultrastructural Research, National Institute of Neuroscience, National Center of Neurology and Psychiatry, Kodaira, Tokyo 187-8502, Japan

²Laboratory for Cortical Organization and Systematics, RIKEN Brain Science Institute, Wako City, Saitama 351-0198, Japan

Inventory of Supplemental Information:

Supplementary information A: **What we are looking at in our *in vivo* SCI.**

Supplementary information B: **Size and distribution of retrograde and anterograde patches.**

Supplementary Information C: **Another potential application of our *in vivo* SCI.**

Supplementary Figure S1 : **Plotted coronal sections of M2.**

Supplementary Figure S2: **Spatial relationship among one feedforward projection (red) and two intrinsic networks (green and silver) in M2. Color-coded flat maps of red, blue, silver neurons, and their combinations.**

Supplementary Figure S3: **Plotted coronal sections of M3.**

Supplementary Figure S4: **Spatial relationship among one feedforward projection (red) and two intrinsic networks (green and silver) in M3. Color-coded flat maps of red, blue, silver neurons, and their combinations.**

Supplementary Figure S5: **SCI after perfusion with experiment of DiI placement.**

Supplementary Figure S6: **Results of an injection of a mixture of three CTB conjugates (CTB-Alexa 488, -Alexa 555, and -gold).**

Supplementary Table S1: **Size of each patch for each tracer in TEO of each monkey.**

Supplementary Table S2: **Summary of size of patches for each tracer in TEO of each monkey.**

Supplementary Table S3: **Summary of center-to-center distance in TEO of each monkey.**

Supplementary Table S4: **Correlation coefficient between numbers of neurons of two colours within each pixel in all whole TEO.**

Supplementary Table S5: **Number of CTB-Alexa 488 and/or -Alexa 555 labeled neurons around CTB-Alexa 488 injection sites on the sections through middle of injection sites**

Supplementary Table S6: **Summary of labeled neurons in each patch and pixel of TEO in M1**

Supplementary Table S7: **Summary of labeled neurons in each patch and pixel of TEO in M2.**

Supplementary Table S8: **Summary of labeled neurons in each patch and pixel of TEO in M3.**

Supplementary Table S9: **Summary of Experiments.**

Supplementary Information A

What we are looking at in our *in vivo* SCI. Because TEO is convoluted in shape, some distortion is inevitable in a 2-dimensional unfolded flat-map. To confirm that *in vivo* and histological patches corresponded, we used DiI (Sigma-Aldrich, St. Louis, MO) in the postmortem brain to mark what had been identified as fluorescent spots *in vivo*. First, to avoid washing out of DiI crystal, after perfusion, the fixed brain was removed and the surface was imaged by fluorescence microscopy, using a filter for red fluorescent protein at a magnification of 5–20×. Patches of red fluorescence were observed within both V4 and TEO, within a triangle bound by the STS, posterior middle temporal sulcus (PMTS), and inferior occipital sulcus (IOS) (case M4 in Supplementary Fig. S5). Second, we locally applied DiI (10% in EtOH) with an electrode tip at the brain surface overlying the fluorescent patches (six positions in TEO and three positions in V4, arrows in Supplementary Fig. S5, white and yellow asterisks in Supplementary Fig. S5). Areas without fluorescence were also marked (three positions in TEO: blue asterisks in Supplementary Fig. S5). Third, brain blocks containing the DiI-labeled areas, including TEO and V4, were cut into coronal sections of 50 μm thicknesses. DiI placed on the fluorescent patches always corresponded to histologically visualized CTB-Alexa555-labeled neurons (red neurons; Supplementary Fig. S5d). We noted that the territories occupied by CTB-Alexa555-labeled neurons in the deep layers were sometimes wider than those in the upper layers. Because of this asymmetry and because the deeper CTB-Alexa555-labeled neurons appeared not to be visible from the surface (Fig. Supplementary S5), we concluded that infragranular neurons do not contribute to the patches of fluorescence at the brain surface. When DiI was placed on areas without

fluorescence, as a control, there were only a few (2-3) underlying CTB-Alexa555-labeled red neurons (Supplementary Fig. S5; blue asterisks).

In another control, we compared the efficacy of the different retrograde tracers within the TE–TEO system by injecting all three tracers at the same site in M5. This resulted in a dense field of triple labeled cells (Supplementary Fig. S6). Therefore, we can conclude that all three tracers were similarly efficient in the TEO–TE system, and did not interfere with each other.

Supplementary Information B

Size and distribution of retrograde and anterograde patches. In general, in TEO the number of green and silver patches in our material was less than the number of patches revealed in other studies by anterograde tracer (anterograde patches: more than 25 patches)¹. Our retrograde patches were 2 times greater in diameter than was reported for anterograde patches (~0.5 μm diameter), about 4 times larger in area than the anterograde patches¹, and the distance between green patches and between silver patches was about twice that for anterograde patches¹. The parameters of our retrogradely based patches in TEO are, however, similar to what has been reported in other studies with retrograde tracer².

References

1. Fujita, I. & Fujita, T. Intrinsic Connections in the macaque inferior temporal cortex. *J. Comp. Neurol.* 368, 467-486 (1996).

2. Felleman, D.J., Xiao, Y. & McClendon, E. Modular organization of occipito-temporal pathways: cortical connections between visual area 4 and visual area 2 and posterior inferotemporal ventral area in macaque monkeys. *J. Neurosci.* 17, 3185-3200 (1997).

Supplementary Information C

Another potential application of our *in vivo* SCI. In this study, we developed an *in vivo* SCI method. There are several noninvasive methods for *in vivo* connection imaging, including enhanced magnetic resonance imaging (e.g., manganese, CTB-conjugated tracers)^{1,2}, but columnar or laminar resolution is so far not optimal with these approaches. In our method, the retrograde patches and the fine network of cortical blood vessels were used as a high-resolution grid (~ less than 100 μm) to guide tracer injections or other needle-like apparatuses (e.g., electrophysiological electrodes, viral vector injections, or light apparatuses for optogenetics).

There have been several previous attempts to develop a way to visualize connectional assemblies *in vivo*. Malach used a different fluorescent tracer, with some problems of toxicity³. Jarosiewicz et al.⁴ used CTB-Alexa555 and Alexa594 combined with two photon Ca imaging to discriminate projection-target specific neuron response properties in cat visual cortex⁴. However, their cranial window was limited (250 x 250 μm^2), and not suitable for visualization of long distance projections. Wang et al. (2007) used anterograde tracers (Fluoro-Ruby and Fluoro-Emerald) to visualize and record from mouse V2⁵. Our method can similarly be used for electrophysiological studies, with simultaneous recordings from two spots connected by patchy dense connections.

Our *in vivo* SCI method can also be used for targeting projection-specific gene expression. Recently, highly efficient retrograde-transport viral vectors^{6,7} have become available, and the combination of these retrograde viral vectors and other vectors or agents (e.g., Tet-on systems and immunotoxin)^{8,9} allow, for example, induction of projection-specific gene expression (e.g., transmission-inhibiting tetanus toxin⁸ and genes such as brain-derived neurotrophic factor), or destruction of projection-specific neurons⁹. As shown here, our *in vivo* SCI method allows visualization of strongly interconnected areas, which can then be injected with different types of vectors or agents to maximize double infections in specific connections.

References

1. Saleem KS, Pauls JM, Augath M, Trinath T, Prause BA, Hashikawa T, Logothetis NK. Magnetic resonance imaging of neuronal connections in the macaque monkey. *Neuron* 34, 685-700 (2002).
2. Wu, C.W., Vasalatiy, O., Liu, N., Wu, H., Cheal, S., Chen, D.Y., Koretsky, A.P., Griffiths, G.L., Tootell, R.B. & Ungerleider, L.G. Development of a MR-visible compound for tracing neuroanatomical connections in vivo. *Neuron* 70, 229-243 (2011).
3. Malach, R. *In vivo* visualization of callosal pathways: a novel approach to the study of cortical organization. *J. Neurosci. Methods* 25, 225-238 (1988).
4. Jarosiewicz, B., Schummers, J., Malik, W.Q., Brown, E.N. & Sur, M. Functional biases in visual cortex neurons with identified projections to higher cortical targets. *Curr. Biol.* 22, 269-277 (2012).
5. Wang, Q., Gao, E. & Burkhalter, A. *In vivo* transcranial imaging of connections in

mouse visual cortex. *Journal of Neuroscience Methods* 159, 268–276 (2007).

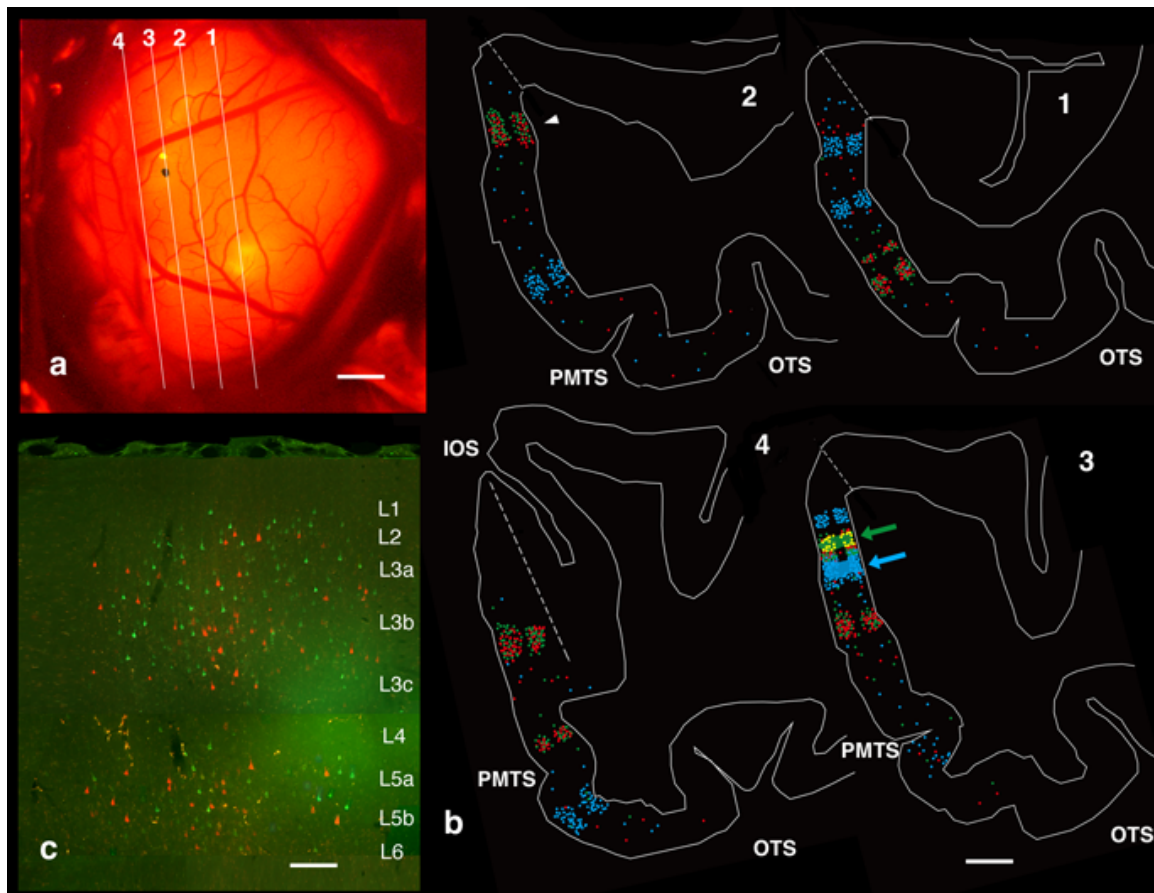
6. Kato, S., Kobayashi, K., Inoue, K., Kuramochi, M., Okada, T., Yaginuma, H., Morimoto, K., Shimada, T., Takada, M., & Kobayashi, K. A lentiviral strategy for highly efficient retrograde gene transfer by pseudotyping with fusion envelope glycoprotein. *Hum. Gene Ther.* 22, 197-206 (2011)..

7. Kato, S., Kuramochi, M., Takasumi, K., Kobayashi, K., Inoue, K., Takahara, D., Hitoshi, S., Ikenaka, K., Shimada, T., Takada, M. & Kobayashi, K. Neuron-specific gene transfer through retrograde transport of lentiviral vector pseudotyped with a novel type of fusion envelope glycoprotein. *Hum. Gene Ther.* 22, 1511-1523 (2011).

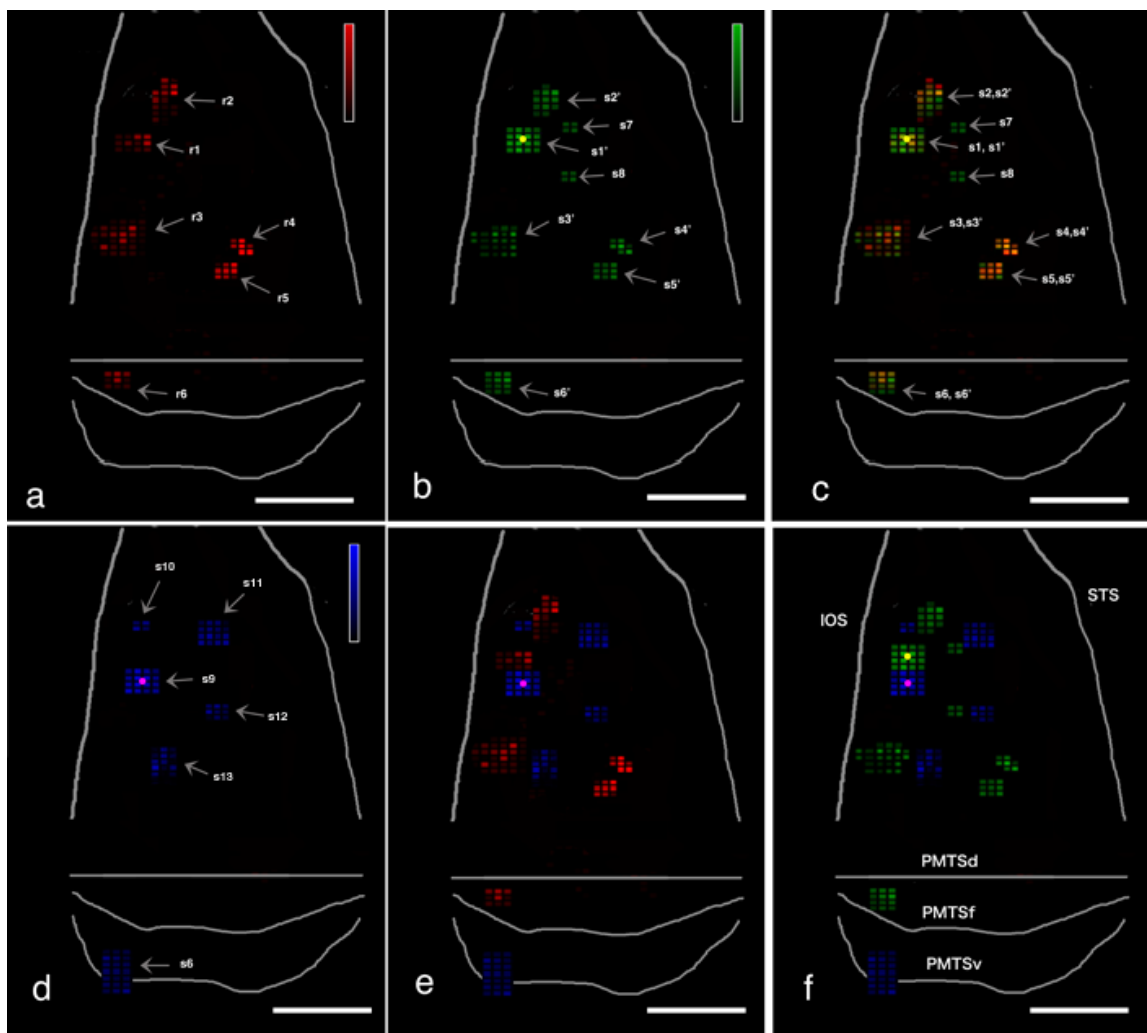
8. Kinoshita, M., Matsui, R., Kato, S., Hasegawa, T., Kasahara, H., Isa, K., Watakabe, A., Yamamori, T., Nishimura, Y., Alstermark, B., Watanabe, D., Kobayashi, K. & Isa T. Genetic dissection of the circuit for hand dexterity in primates. *Nature* 487, 235-238 (2012).

9. Inoue, K., Koketsu, D., Kato, S., Kobayashi, K., Nambu, A. & Takada M. Immunotoxin-mediated tract targeting in the primate brain: selective elimination of the cortico-subthalamic "hyperdirect" pathway. *PLoS One* 7, e39149 (2012).

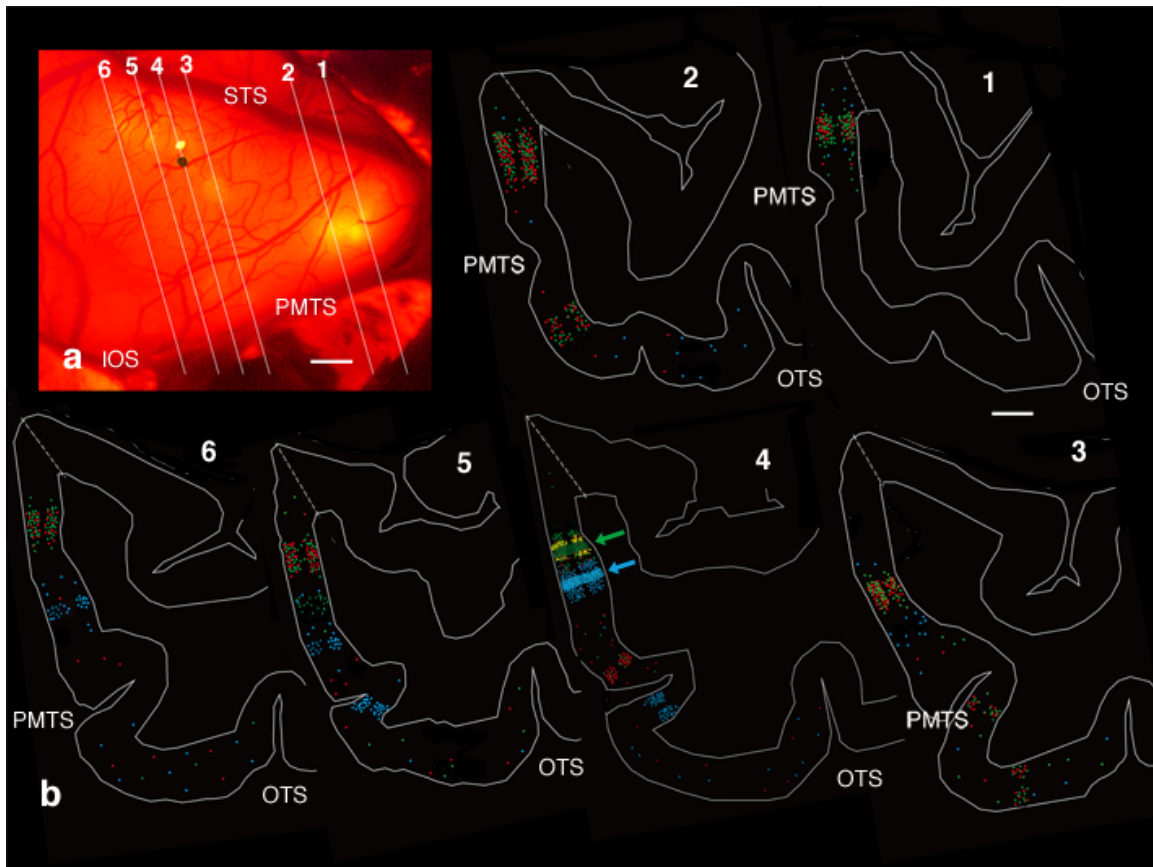
Supplementary Figure S1| Plotted coronal sections of M2. (a) Coronal section lines superimposed on *in vivo* SCI, and corresponding to the tissue sections in b. (b) Plots of labeled neurons, in coronal sections (only ventral portion is shown) from the field shown in (a). Red, green and blue circles represent red, green and silver neurons. Plotting was limited to TEO. Arrows point to injection sites of green and silver tracers. Arrowhead at upper left section points to the overlapping patch shown at higher magnification in (c). (c) Intermingled red and green neurons from the arrowhead in (b). Scale bar represents 1 mm (a), 1.5 mm (b), 250 μ m (c).



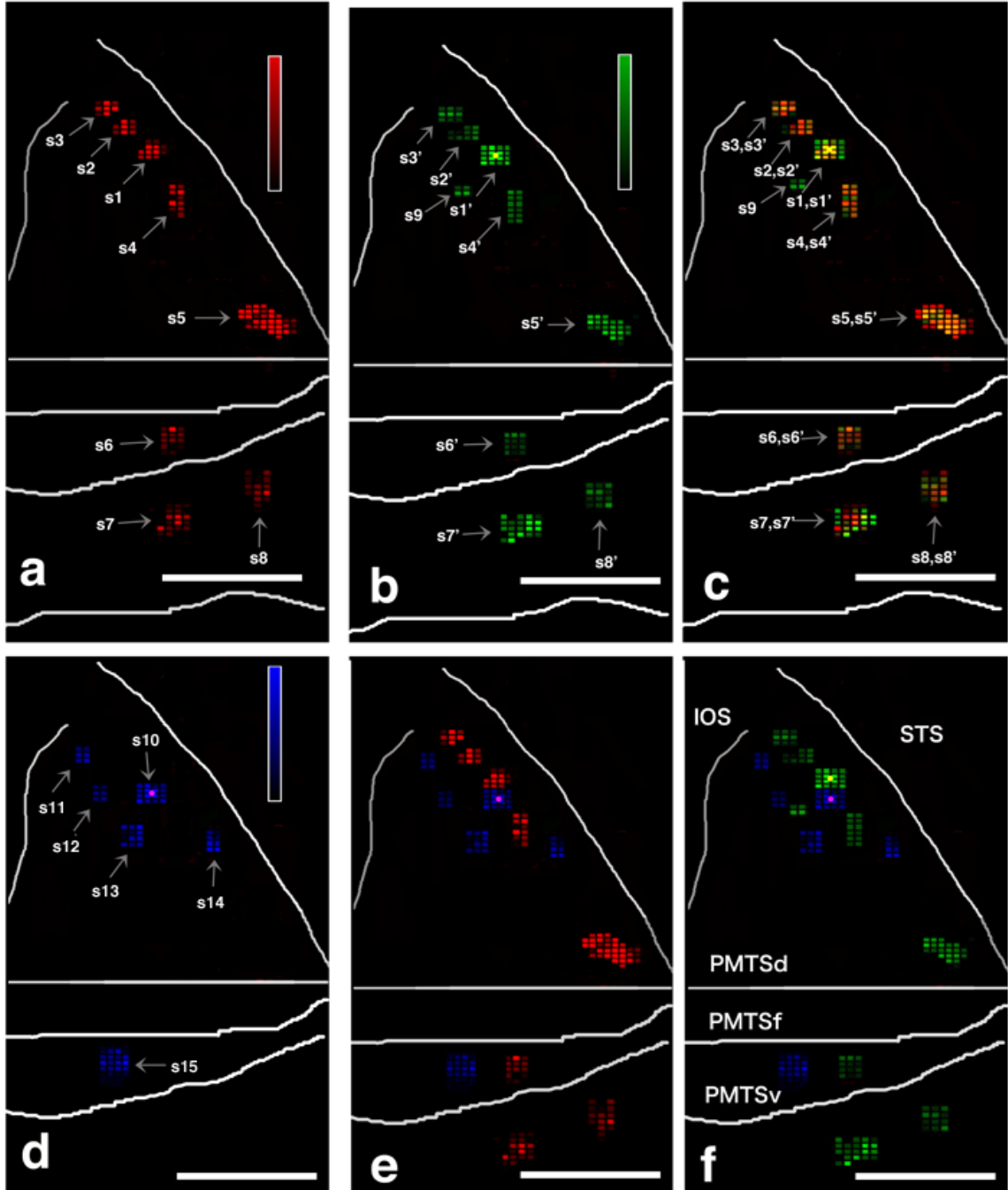
Supplementary Figure S2| Spatial relationship of one feedforward projection (red) and two intrinsic networks (green and silver) in M2, shown as flat map. Color-coded flat maps of red (a) and green neurons (b), and their merge (c), silver neurons, colorized to blue for the sake of better contrast (d), merge of red and silver (shown as blue) neurons (e) and merge of green and blue neurons (f). CTB-Alexa488 injection sites are yellow filled circle in b, c, and f, and CTB-Gold are purple dots in d, e, and f. For abbreviations, scale bar and Heat map scale of density of a pixel, see fig. 4.



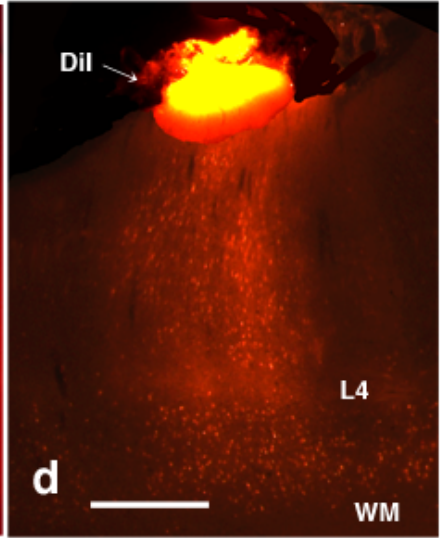
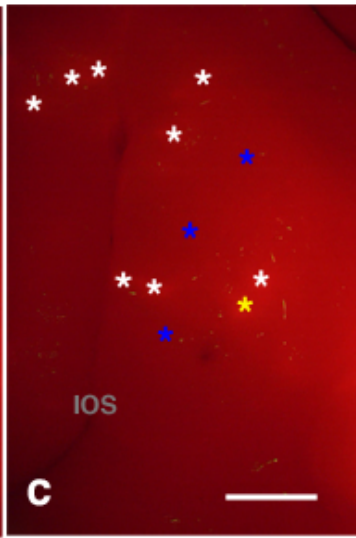
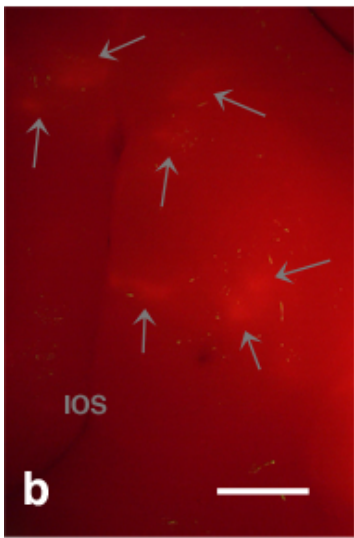
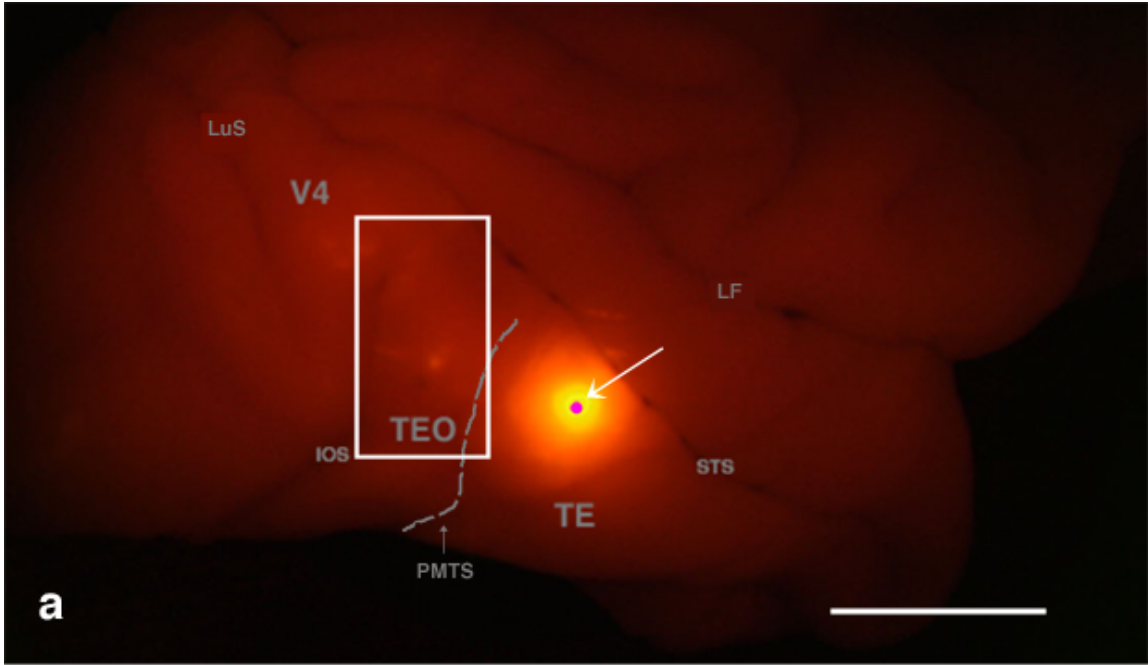
Supplementary Figure S3| Plotted coronal sections of M3. (a) Coronal section lines superimposed on *in vivo* SCI, and corresponding to the tissue sections in b. (b) Plots of labeled neurons, in coronal section (only ventral is shown) from the field shown in (a). Red, green and blue circles represent red, green and silver neurons. Plotting was limited to TEO. Arrows point to injection sites of green and silver (shown as blue) tracers. Scale bar represents 1 mm (a), 500 μ m (b).



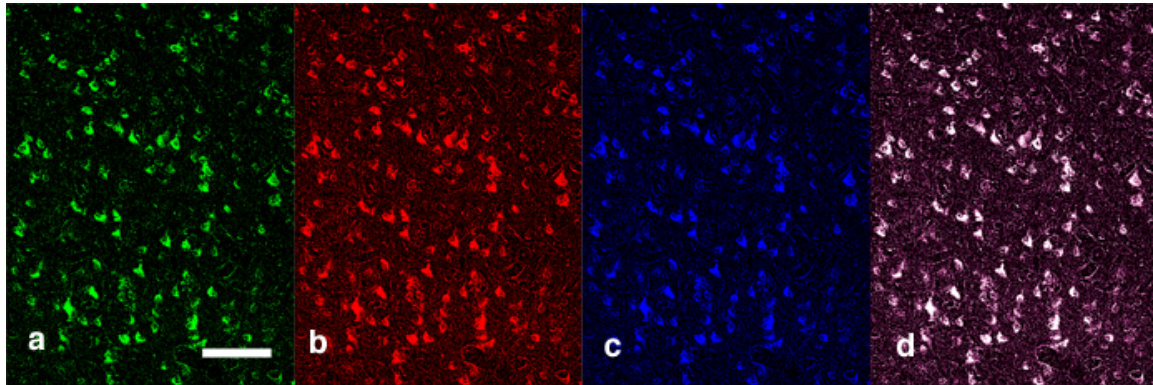
Supplementary Figure S4| Spatial relationship of one feedforward projection (red) and two intrinsic networks (green and silver) in M3, shown as flat map. Color-coded flat maps of red (a) and green neurons (b), and their merge (c); silver neurons (expressed as blue) (d), merge of red and silver (blue) neurons (e), and merge of green and silver (blue) neurons (f). CTB-Alexa488 injection sites are yellow filled circle in b, c, and f, and CTB-Gold are purple dots in d, e, and f. For abbreviations, scale bar and Heat map scale of density of a pixel, see fig. 4.



Supplementary Figure S5| SCI of a perfused postmortem brain, prepared for DiI placement. (a) An example of fluorescent SCI of the fixed brain (M4). The injection site of CTB-Alexa555 (arrow) is surrounded by a bright fluorescent halo. The rectangle indicates the area containing fluorescent spots in TEO and part of V4. (b) An enlarged image of the spots (at arrows). (c) The same image as (b). The asterisks represent the positions of DiI application (white and yellow asterisks = DiI positioned on fluorescence spots, and blue asterisks = DiI positioned off fluorescence spots). (d) Coronal section through the DiI application site (yellow asterisk) in c. Under the DiI-labeled patch, there are numerous CTB-Alexa555-labeled neurons. Note that the neurons are more widespread in the lower layers. Abbreviations: IOS, inferior occipital sulcus; L4, layer 4; LF, lateral fissure; LuS, lunate sulcus; PMTS, posterior middle-temporal sulcus; STS, superior temporal sulcus; TE, area TE; TEO, area TEO; V4, area V4; WM, white matter. Scale bar represent 1 mm (a), 200 μ m (b, c), and 50 μ m (d).



Supplementary Figure 6| Results of an injection of a mixture of three CTB conjugates (CTB-Alexa488, -Alexa555, and -gold). (a) Photograph of a field of CTB-Alexa488-labeled neurons, at 5 mm from the injection site, (b) Same, for CTB-Alexa555, (c) Same, for pseudo-coloured (blue) CTB-gold enhanced by silver, (d) Merged image of (a), (b) and (c). Scale Bar represents 100 μm .



Supplementary Table S1. Size of patch size for each tracer in TEO of M1, M2, M3

M1										
red*(patch#=9)	r1	r2	r3	r4	r5	r6	r7	r8	r9	
X axis (mm) [±]	2.5	0.75	0.75	0.5	1.5	1.0	0.75	0.5	1.0	
Y axis (mm) [±]	2.75	1.25	0.75	1.0	1.5	0.5	1.5	1.5	1.25	
Area (mm ²)	6.75	3.75	0.75	2.25	1.0	1.0	1.25	1.0	1.0	
green*(patch#=10)	g1	g2	g3	g4	g5	g6	g7	g8	g9	g10
X axis (mm) [±]	2.5	0.75	0.75	0.5	1.5	1.0	0.75	0.5	1.0	0.5
Y axis (mm) [±]	2.75	1.25	0.75	1.0	1.5	0.5	1.5	1.5	1.25	0.5
Area (mm ²)	6.75	3.75	0.75	2.25	1.0	1.0	1.25	1.0	1.0	0.06
silver*(patch#=8)	s1	s2	s3	s4	s5	s6	s7	s8		
X axis (mm) [±]	1.0	0.75	0.75	0.75	0.75	0.5	0.5	0.75		
Y axis (mm) [±]	1.0	1.0	1.0	1.25	1.0	1.5	0.75	1.0		
Area (mm ²)	1.0	1.0	0.6	0.6	0.5	0.7	0.4	0.5		

M2										
red*(patch#=6)	r1	r2	r3	r4	r5	r6				
X axis (mm) [±]	1.0	0.75	1.5	0.75	0.75	0.75				
Y axis (mm) [±]	1.0	1.75	1.5	0.75	0.75	0.75				
Area (mm ²)	1.0	2.0	2.75	1.0	1.13	1.5				
green*(patch#=8)	g1	g2	g3	g4	g5	g6	g7	g8		
X axis (mm) [±]	1.0	0.75	1.5	0.75	0.75	0.75	0.5	0.5		
Y axis (mm) [±]	1.0	1.75	1.5	0.75	0.75	0.75	0.5	0.5		
Area (mm ²)	1.0	2.0	2.75	1.0	1.13	1.5	0.25	0.25		
silver*(patch#=6)	s1	s2	s3	s4	s5	s6				
X axis (mm) [±]	1.0	0.5	1.0	0.75	0.75	0.75				
Y axis (mm) [±]	1.0	0.5	1.0	0.5	1.25	0.75				
Area (mm ²)	1.0	0.25	1.0	0.6	0.75	1.31				

M3										
red*(patch#=8)	r1	r2	r3	r4	r5	r6	r7	r8		
X axis (mm) [±]	1.0	0.75	0.75	0.50	2.0	0.75	1.0	0.75		
Y axis (mm) [±]	1.0	0.75	0.75	2.0	1.75	1.25	1.5	1.5		
Area (mm ²)	1.0	2.0	2.75	1.0	1.13	1.5				
green*(patch#=9)	g1	g2	g3	g4	g5	g6	g7	g8	g9	
X axis (mm) [±]	1.0	0.75	0.75	0.75	0.75	0.75	0.75	0.75	0.5	
Y axis (mm) [±]	1.0	0.75	0.75	0.75	0.75	0.75	0.75	0.75	0.5	
Area (mm ²)	1.0	2.0	2.75	1.0	1.13	1.5	0.25	0.25	0.25	
silver*(patch#=6)	s1	s2	s3	s4	s5	s6				
X axis (mm) [±]	1.0	0.5	0.5	0.75	0.5	1.0				
Y axis (mm) [±]	1.0	0.75	0.75	1.0	1.0	1.5				
Area (mm ²)	1.0	0.25	1.0	0.6	0.75	1.31				

Abbreviations: red*, CTB-Alexa 555 labeled patch; green*, CTB-Alexa 448 labeled patch; silver*, CTB-gold-labeled patch. In this table, patch was defined by histologically. See Results section for definition of histological patches; r + Arabic number, red patch + Arabic number; g + Arabic number, green patch + Arabic number; s + Arabic number, silver patch + Arabic number (see Figure 2, 6, 3S, 5S); X axis is an axis along with dorsal bank of PMTS in 2 dimensional unfolded maps. Y axis is an axis perpendicular to X axis.

Supplementary Table S2. Summary of patch size for each tracer in TEO of M1, M2, and M3

M1					
	Mean	STD	Median	Maximum	Minimum
red* (9 patches)					
[±] long axis (mm) [±]	1.40	0.58	1.25	2.75	0.75
[±] short axis (mm) [±]	0.97	0.66	0.75	2.50	0.50
Area (mm ²)	2.10	2.00	1.0	6.75	0.75
green* (10 patches)					
[±] long axis (mm) [±]	1.30	0.61	1.25	2.75	0.50
[±] short axis (mm) [±]	0.93	0.64	1.25	2.50	0.50
Area (mm ²)	1.98	1.90	1.0	6.75	0.75
silver* (7 patches)					
[±] long axis (mm) [±]	1.06	0.22	1.00	1.50	0.75
[±] short axis (mm) [±]	0.72	0.16	0.75	1.00	0.50
Area (mm ²)	0.61	0.20	0.56	1.00	0.38

Abbreviation: Red*, CTB-Alexa555 labeled patches; green*, CTB-Alexa448 labeled patches; silver*, CTB-gold-labeled patches.

[±]: Long and short axis are longer or shorter axis comparing X and Y axis. X axis is an axis along with dorsal bank of PMTS in 2 dimensional unfolded maps. Y axis is an axis perpendicular to X axis.

M2					
	Mean	STD	Median	Maximum	Minimum
red* (6 patches)					
[±] long axis (mm) [±]	1.08	0.44	0.75	1.75	0.75
[±] short axis (mm) [±]	0.88	0.31	0.75	1.50	0.75
Area (mm ²)	1.56	0.7	1.31	2.75	1.0
green* (8 patches)					
[±] long axis (mm) [±]	0.91	0.35	0.88	1.5	0.50
[±] short axis (mm) [±]	0.78	0.25	0.75	1.25	0.50
Area (mm ²)	1.23	0.84	1.06	2.75	0.25
silver* (6 patches)					
[±] long axis (mm) [±]	1.08	0.52	1.00	2.00	0.50
[±] short axis (mm) [±]	0.75	0.22	0.75	1.00	0.50
Area (mm ²)	0.81	0.38	0.86	1.31	0.25

M3					
	Mean	STD	Median	Maximum	Minimum
red* (6 patches)					
[±] long axis (mm) [±]		0.47	1.50	2.00	0.75
[±] short axis (mm) [±]	1.50	0.43	0.75	1.75	0.75
Area (mm ²)	1.08	1.45	1.44	4.63	1.0
green* (8 patches)	2.03				
[±] long axis (mm) [±]		0.47	0.75	1.5	0.50
[±] short axis (mm) [±]	1.11	0.44	0.65	1.25	0.50
Area (mm ²)	0.82	1.48	1.25	4.63	0.25
silver* (6 patches)	1.83				
[±] long axis (mm) [±]		0.31	1.00	1.50	0.50
[±] short axis (mm) [±]	1.13	0.25	0.63	1.00	0.50
Area (mm ²)	0.81	0.36	0.50	1.13	0.25
	0.63				

Supplementary Table S3. Summary of distance among the same colored patches in whole TEO area

The center-to-center distance between a patch and all of its surrounding neighbors (mm) Mean \pm SD	The distance to the nearest neighbor from each patch (mm) Mean \pm SD
M1	
red* (9 patches)	
2.90 \pm 0.95	1.62 \pm 0.50
green* (10 patches)	
2.98 \pm 1.05	1.70 \pm 0.51
silver* (7 patches)	
3.10 \pm 0.75	1.81 \pm 0.42
M2	
red* (6 patches)	
3.02 \pm 0.98	1.67 \pm 0.52
green* (8 patches)	
3.15 \pm 1.01	1.72 \pm 0.58
silver* (6 patches)	
3.20 \pm 0.95	1.82 \pm 0.53
M3	
red* (6 patches)	
3.30 \pm 1.15	1.72 \pm 0.53
green* (8 patches)	
3.40 \pm 1.22	1.78 \pm 0.57
silver* (6 patches)	
3.31 \pm 1.05	1.68 \pm 0.52

red*, CTB-Alexa555 labeled patches; green*, CTB-Alexa448 labeled patches; silver*, CTB-gold-labeled patches.

Supplementary Table S4. Correlation coefficient between numbers of two different colors of neurons in a each pixel in all whole TEO area.

Correlation Coefficeint (<i>r</i>)
M1 (1121 pixels examined)
Red and Green
0.97***
Red and Silver
-0.63**
Green and Silver
-0.61**
M2 (1246 pixels examined)
Red and Green
0.93***
Red and Silver
-0.60**
Green and Silver
-0.60**
M3 (1296 pixels examined)
Red and Green
0.96***
Red and Silver
-0.60**
Green and Silver
-0.56**

red*, CTB-Alexa 555 labeled patches; green*, CTB-Alexa 448 labeled patches; silver*, CTB-gold-labeled patches.

***: $p < 0.01$ (positive statistical significance by Spearman's rank correlation coefficient)

** : $p < 0.01$ (negative statistical significance by Spearman's rank correlation coefficient)

Supplementary Table S5: Number of CTB-Alexa 488 and/or Alexa 555 labeled neurons near CTB-Alexa 488 injection sites (from center to 250 μm and the area between 250 μm and 500 μm).

Distance from center of CTB-Alexa 488 injection site	250 μm	250 -500 μm	250 μm	250-500 μm	250 μm	250-500 μm
monkey	M1		M2		M3	
SGL						
Red (r)	125	130	114	92	103	140
green (g)	3110	140	2159	127	3028	152
DL(r+g)	103	8	91	5	100	9
total	3338	278	2365	225	3231	302
DL(r+g)/total (%)	3	3	4	2	3	3
DL(r+g)/g (%)	3	6	4	4	3	6
DL(r+g)/r (%)	82	6	79	6	97	7
IGL						
red (r)	38	43	32	27	32	45
green (g)	843	42	675	38	934	49
DL(r+g)	32	2	29	2	30	3
total	914	87	736	66	996	97
DL(r+g)/total (%)	4	3	4	2	3	3
DL(r+g)/g (%)	4	6	4	4	3	5
DL(r+g)/r (%)	84	6	91	6	96	6

Abbreviations: g, number of green neurons; DL (r+g), number of neurons double-labeled by red and green; IGL, infragranular layer, number of red neurons; SGL, supragranular layer; total, r+g.

Supplementary Table S6: Summary of labeled neurons in each red/green overlapped patch and pixel of TEO in M1.

	Total	r1, g1	r2, g2	r3, g3	r4, g4	r5, g5	r6, g6	r7, g7	r8, g8	r9, g9	Summary of each pixel	means	SD	Median	maximum	minimum
Number of pixels	167	59	30	6	18	8	8	10	9	6						
Layer 2																
r	1192	450	244	50	132	69	59	82	60	45		7.14	0.62	7	10	0
g	1873	700	367	72	235	94	104	122	103	77		11.21	0.97	11	16	0
DL(r+g)	2	1	1	0	0	0	0	0	0	0		0.01	0	0	2	0
total	3067	1151	612	122	367	163	163	204	163	122		18.36	1.65	17	26	5
DL(r+g) /total (%)	0.07	0.09	0.16	0.00	0.00	0.00	0.00	0.00	0.00	0.00		0.07	0.00	0.07	0.14	0.00
r/(r+g)(%)	38	39	40	41	36	43	36	40	37	37		39	0.07	0.40	0.56	0.00
Layer 3a																
r	2667	892	577	122	326	151	144	192	149	112		15.97	1.22	15	30	5
g	2491	990	468	87	301	127	135	156	130	97		14.92	1.45	15	32	7
DL(r+g)	6	2	1	1	0	1	1	0	0	0		0.04	0	0	4	0
total	5164	1884	1047	210	627	280	280	349	279	209		30.92	2.7	30	42	21
DL(r+g) /total (%)	0.12	0.11	0.10	0.48	0.00	0.36	0.36	0.00	0.00	0.00		0.12	0	0	0.18	0
r/(r+g)(%)	51	47	55	59	52	54	52	55	54	54		52	11.00	45.00	71.00	25.00
Layer 3b																
r	2526	900	489	117	292	152	133	203	137	102		15.13	0.10	15.00	42.00	10.00
g	2687	1002	568	94	342	130	149	149	145	109		16.09	1.22	16	35	8
DL(r+g)	2	3	2	0	1	1	0	1	1	1		0.06	0	0	4	0
total	5225	1905	1059	212	635	283	282	354	283	212		31.29	1.38	31	55	21
DL(r+g) /total (%)	0.19	0.16	0.19	0.00	0.16	0.35	0.00	0.28	0.35	0.47		0.19	0	0	0.23	0
r/(r+g)(%)	49	47	46	56	46	54	47	58	48	48		48	4.00	48	60	30
Layer 3c																
r	3124	1200	684	113	346	187	152	178	151	113		18.71	0.10	18.00	28.00	10.00
g	2906	1000	539	132	387	139	174	229	175	131		20.27	1.68	20	34	12
DL(r+g)	11	5	2	1	1	0	1	0	1	0		0.07	0	0	1	0
total	6045	2206	1224	245	734	327	328	407	328	244		36.20	1.25	36	51	26
DL(r+g) /total (%)	0.18	0.23	0.16	0.41	0.14	0.00	0.30	0.00	0.30	0.00		0.18	0	0	0.21	0
r/(r+g)(%)	51	55	56	46	47	57	47	44	46	46		48.00	4.23	48	60	38
Layer 5a																
r	1446	520	295	59	177	79	79	98	79	59		8.66	0.72	9	13	4
g	1569	580	316	63	189	84	84	105	84	63		9.38	0.80	9	11	4
DL(r+g)	4	2	2	0	0	0	0	0	0	0		0.02	0	0	1	0
total	3020	1103	613	122	367	163	163	204	163	122		18.08	1.72	18	38	12
DL(r+g) /total (%)	0.13	0.18	0.33	0.00	0.00	0.00	0.00	0.00	0.00	0.00		0.13	0	0	0.20	0
r/(r+g)(%)	48	47	48	48	48	48	48	48	48	48		48.00	5.01	0.48	0.63	0.32
Layer 5b																
r	1662	610	336	67	201	90	90	112	90	67		9.95	0.84	4	6	3
g	1764	640	359	72	215	96	96	120	96	72		10.56	0.81	5	6	3
DL(r+g)	3	2	1	0	0	0	0	0	0	0		0.02	0	0	1	0
total	3428	1252	694	139	417	185	185	231	185	139		20.53	2.00	25	31	17
DL(r+g) /total (%)	0.09	0.16	0.14	0.00	0.00	0.00	0.00	0.00	0.00	0.00		0.09	0	0	0.15	0
r/(r+g)(%)	48	49	48	48	48	48	48	48	48	48		49	5.02	0.49	0.64	0.34
Layer 6																
r	1634	600	351	71	183	89	82	109	85	64		9.79	0.77	4	6	3
g	1710	620	327	65	224	92	98	116	95	72		10.24	0.82	4	6	3
DL(r+g)	4	3	1	0	0	0	0	0	0	0		0.02	0	0	1	0
total	3347	1223	678	136	407	181	181	226	181	136		20.04	1.85	20	32	12
DL(r+g) /total (%)	0.12	0.25	0.15	0.00	0.00	0.00	0.00	0.00	0.00	0.00		0.12	0	0	0.20	0
r/(r+g)(%)	50	49	52	52	45	49	46	48	47	47		49	5.12	0.49	0.65	0.34
Whole Layer																
r	11725	4272	2487	482	1367	665	606	772	614	461		70.21	7.50	70	90	58
g	14999	5532	2943	584	1892	761	840	998	828	621		89.82	8.01	90	105	75
DL(r+g)	40	18	10	2	2	2	2	1	2	1		0.24	0.00	0	1	0
total	29295	10724	5927	1187	3553	1581	1581	1975	1581	1185		175.42	17.54	176	200	151
DL(r+g) /total (%)	0.14	0.17	0.17	0.17	0.06	0.13	0.13	0.05	0.13	0.08		0.14	0.00	0	0.20	0
r/(r+g)(%)	47	44	46	45	42	47	42	44	43	43		44	4.21	44	54	34

Abbreviations: DL(r+g), number of neurons double-labeled for red and green; g, number of green neuron; g+number, green patch number; r, number of red neurons; r+number, red patch number; total, r+g.

Supplementary Table S7: Summary of labeled neurons in each red/green overlapped patch and pixel of TEO in M2.

	Total	r1, g1	r2, g2	R3, g3	r4, g4	r5, g5	r6, g6	Summary of each pixel	means	SD	Median	maximum	minimum
Number of pixels	167	0	16	22	8	9	12						
Layer 2													
r	540	0	103	159	49	70	78		3.24	0.28	3	5	1
g	906	0	223	290	114	113	167		5.43	0.42	5	8	2
DL(r+g)	1	0	0	0	1	0	0		1	0	0	1	0
total	1450	0	326	448	163	183	244		8.68	1.65	17	26	5
DL(r+g) /total (%)	0.07	0	0.00	0.00	0.61	0.00	0.00		0.07	0	0.07	0.14	0.00
r/(r+g)(%)	37	0	32	35	30	38	32		37	0.07	0.40	0.56	0.00
Layer 3a													
r	3039	0	300	405	125	178	204		18.20	1.22	18	30	10
g	2886	0	257	362	153	136	214		17.28	1.45	17	32	7
DL(r+g)	6	0	1	1	1	2	1		4	0	0	4	0
total	5936	0	561	768	281	318	419		35.54	2.7	35	42	21
DL(r+g) /total (%)	0.10	0	0.18	0.13	0.36	0.63	0.24		0.10	0	0	0	0
r/(r+g)(%)	51	0	54	53	45	57	49		51	11.00	45.00	71.00	25.00
Layer 3b													
r	2923	0	243	437	127	195	247		17.50	1.40	18.00	25.00	9.00
g	3064	0	320	338	155	122	176		18.35	1.22	18	28	10
DL(r+g)	6	0	2	1	2	0	1		0.04	0	0	4	0
total	5988	0	564	775	282	317	423		35.85	1.38	36	51	25
DL(r+g) /total (%)	0.10	0	0.35	0.13	0.71	0.00	0.24		0.10	0	0	0	0
r/(r+g)(%)	49	0	43	56	45	61	58		49	4.00	48	60	30
Layer 3c													
r	3510	0	387	534	194	217	241		21.02	1.60	21.00	31.00	11.00
g	3416	0	265	362	132	150	248		22.77	1.68	23	33	12
DL(r+g)	9	0	1	2	2	2	2		0.05	0	0	1	0
total	6926	0	652	896	326	367	489		41.47	1.25	43	72	20
DL(r+g) /total (%)	0.13	0	0.15	0.22	0.61	0.55	0.41		0.13	0	0	0	0
r/(r+g)(%)	51	0	59	60	59	59	49		48.00	4.23	48	60	38
Layer 5a													
r	1662	0	182	250	91	102	136		9.95	0.72	10	15	6
g	1801	0	194	267	97	109	146		10.78	0.80	11	16	7
DL(r+g)	4	0	1	0	2	1	0		0.02	0	0	1	0
total	3463	0	376	517	188	212	282		20.74	1.72	21	36	12
DL(r+g) /total (%)	0.12	0	0.27	0.00	1.06	0.47	0.00		0.12	0	0	0.18	0
r/(r+g)(%)	48	0	48	48	48	48	48		48.00	5.01	0.48	0.63	0.32
Layer 5b													
R	1908	0	155	213	77	87	116		11.43	0.84	12	18	6
G	2027	0	165	227	83	93	124		12.14	0.81	12	17	6
DL (R + G)	8	0	2	1	2	2	1		0.05	0	0	1	0
Total	3935	0	320	440	160	180	240		23.56	2.00	25	31	17
DL (R + G) /total (%)	0.20	0	0.63	0.23	1.25	1.11	0.42		0.20	0	0	0	0
R/(R+G)(%)	48	0	48	48	48	48	48		48	5.02	49.00	64.00	34.00
Layer 6													
r	1913	0	175	272	86	108	135		11.46	0.77	12	19	4
g	1928	0	187	225	95	96	136		11.54	0.82	12	18	5
DL(r+g)	4	0	0	1	0	1	2		0.02	0	0	1	0
total	3841	0	361	497	181	203	271		23.00	1.85	23	32	12
DL(r+g) /total (%)	0.10	0	0.00	0.20	0.00	0.49	0.74		0.10	0	0	0	0
r/(r+g)(%)	50	0	48	55	47	53	50		50	5.12	0.49	0.65	0.34
Whole Layer													
r	12573	0	1545	2268	749	956	1157		75.29	7.50	70	90	58
g	12963	0	1612	2072	829	819	1210		77.62	8.01	90	105	75
DL(r+g)	32	0	5	5	8	8	6		0.19	0.00	0	1	0
total	25536	0	3156	4340	1578	1776	2367		152.91	17.54	176	200	151
DL(r+g) /total (%)	0.13	0	0.16	0.12	0.51	0.45	0.25		0.13	0.00	0	0	0
r/(r+g)(%)	49	0	49	52	47	54	49		49	4.21	44	54	34

Abbreviations: see Supplementary Table S7.

Supplementary Table S8: Summary of labeled neurons in each red/green overlapped patch and pixel of TEO in M3.

	Total	r1,g1	r2,g2	r3,g3	r4,g4	r5,g5	r6,g6	r7,g7	r8,g8	Summary of each pixel	means	SD	Median	maximum	minimum
Number of pixels	122	0	8	8	14	37	10	32	13						
Layer 2															
r	725	0	44	49	74	226	52	208	74		5.94	0.41	3	7	0
g	1716	0	119	114	211	528	151	444	147		14.07	1.25	6	13	0
DL(r+g)	3	0	0	0	1	1	0	1	0		0.02	0.00	0	1	0
total	2441	0	163	163	285	754	204	652	221		20.01	1.85	20	26	14
DL(r+g)/total (%)	0.12	0	0.00	0.00	0.35	0.13	0.00	0.15	0.00		0.12	0.00	0.14	0.18	0.00
r/(r+g)(%)	30	0	0.27	0.30	0.26	0.30	0.26	0.32	0.28		30	2.52	0.30	0.56	0.00
Layer 3a															
r	1748	0	139	160	247	689	163	208	142		14.33	1.13	4	6	2
g	1824	0	140	119	241	600	185	444	95		14.95	1.35	4	8	2
DL(r+g)	5	0	0	0	0	2	1	1	1		0.04	0.00	0	1	0
total	3572	0	279	279	488	1290	349	652	236		29.28	2.81	30	36	24
DL(r+g)/total (%)	0.14	0	0.35	0.13	0.00	0.15	0.00	0.00	0.00		0.14	0.00	0.14	0.26	0.07
r/(r+g)(%)	49	0	0.50	0.57	0.51	0.53	0.47	0.60	0.54		49	4.23	0.48	0.71	0.25
Layer 3b															
r	1732	0	156	158	245	659	164	208	142		14.19	1.14	14	20	7
g	1869	0	126	124	248	644	188	444	95		15.32	1.29	15	18	7
DL(r+g)	3	0	0	0	0	2	1	0	0		0.02	0	0	1	0
total	3600	0	282	282	493	1303	352	652	236		29.51	2.72	30	37	23
DL(r+g)/total (%)	0.08	0	0.35	0.13	0.00	0.15	0.00	0.00	0.00		0.08	0.00	0.08	0.14	0.07
r/(r+g)(%)	48	0	0.55	0.56	0.50	0.51	0.47	0.65	0.54		48	4.10	48.00	54.00	42.00
Layer 3c															
r	2183	0	168	178	303	963	241	208	121		17.89	1.56	5	8	3
g	1838	0	158	148	267	544	166	444	110		15.06	1.16	4	6	2
DL(r+g)	6	0	0	1	1	2	1	1	0		0.05	0.00	0	1	0
total	4021	0	326	326	570	1507	407	652	232		32.96	3.01	33	40	24
DL(r+g)/total (%)	0.15	0	0.35	0.13	0.00	0.15	0.00	0.00	0.00		0.15	0.00	0.15	0.20	0.07
r/(r+g)(%)	54	0	0.52	0.54	0.53	0.64	0.59	0.49	0.46		54	4.80	54.00	60.00	0.30
Layer 5a															
r	1039	0	79	79	138	364	98	208	74		8.52	0.67	9	13	6
g	1402	0	84	84	147	389	105	444	147		11.49	0.74	12	17	6
DL(r+g)	4	0	0	0	1	2	0	1	0		0.03	0.00	0	1	0
total	2441	0	163	163	285	754	204	652	221		20.01	1.86	20	26	13
DL(r+g)/total (%)	0.16	0	0.35	0.13	0.00	0.15	0.00	0.00	0.00		0.16	0.00	0.16	0.20	0.08
r/(r+g)(%)	43	0	0.48	0.48	0.48	0.48	0.48	0.48	0.48		43	0.07	0.43	0.63	0.32
Layer 5b															
r	1143	0	90	90	157	414	112	208	74		9.37	0.78	9	15	3
g	1512	0	96	96	167	442	120	444	147		12.39	0.75	12	18	4
DL(r+g)	5	0	0	0	1	2	0	2	0		0.04	0.00	0	1	0
total	2655	0	185	185	324	856	231	652	221		21.76	2.02	22	29	18
DL(r+g)/total (%)	0.19	0	0.35	0.13	0.00	0.15	0.00	0.00	0.00		0.19	0.00	0.19	0.23	0.16
r/(r+g)(%)	43	0	0.48	0.48	0.48	0.48	0.48	0.48	0.48		43	4.10	0.49	0.64	0.34
Layer 6															
r	1151	0	84	87	147	426	126	208	74		9.43	0.72	9	16	5
g	1461	0	97	94	170	410	100	444	147		11.98	0.76	12	19	6
DL(r+g)	7	0	0	0	1	3	1	2	0		0.06	0.00	0	1	0
total	2612	0	181	181	316	836	226	652	221		21.41	2.05	22	27	16
DL(r+g)/total (%)	0.27	0	0.35	0.13	0.00	0.15	0.00	0.00	0.00		0.27	0.00	0.27	0.37	0.19
r/(r+g)(%)	44	0	0.47	0.48	0.46	0.51	0.56	0.56	0.47		44	0.07	0.43	0.65	0.34
Whole Layer															
r	7973	0	621	639	1063	3052	794	1245	557		65.35	11.92	65	90	36
g	9798	0	679	660	1211	2958	830	2666	793		80.31	13.25	80	110	56
DL(r+g)	28	0	0	1	5	12	3	7	0		0.23	0.00	0	1	0
total	17770	0	1300	1300	2274	6010	1624	3911	1351		145.66	27.50	145.00	190.00	105.00
DL(r+g)/total (%)	0.16	0	0.00	0.08	0.22	0.20	0.18	0.18	0.00		0.16	0.00	0.14	2.10	0.12
r/(r+g)(%)	45	0	0.48	0.49	0.47	0.51	0.49	0.52	0.41		45	4.1	46	50	42

Abbreviations: see Supplementary Table S7.

Supplementary Table S9: Summary of Experiments.

Monkey	Injection sites and how to determine these sites			Remarks
	CTB-Alexa 555	CTB-Alexa 488	CTB-gold	
M1	TE Using sulcal landmark	TEO Bright spots in <i>in vivo</i> SCI image	TEO Dark parts in <i>in vivo</i> SCI image	CTB-Alexa488 and -gold placement was determined with <i>in vivo</i> SCI
M2	Same as above	Same as above	Same as above	Same as above
M3	Same as above	Same as above	Same as above	Same as above
M4	TE Using sulcal landmarks	Not used	Not used	With DiI placed on bright spots after perfusion
M5	TE Using sulcal landmarks	TE Using sulcal landmarks	TE Using sulcal landmarks	Mixture of three tracers was injected

Abbreviations: CTB, cholera toxin subunit B; SCI, surface connection imaging.